LPM-based NLI Estimation over Heterogeneous Links: Analysis and Comparison

LPM-Based NLI Estimation Over Heterogeneous Links: Analysis and Comparison

Dario Pilori, *Senior Member, IEEE*, Stefano Straullu, *Senior Member, IEEE*, Antonino Nespola, Stefano Piciaccia, and Gabriella Bosco, *Fellow, IEEE*

***Abstract*—Accurate estimation of Non-Linear Interference (NLI) is critical for optimizing ultra-wideband optical networks. This paper investigates the performance of Longitudinal Power Monitoring (LPM)-based NLI estimation, focusing on heterogeneous links. While LPM offers robust, link-agnostic estimation of Self-Channel Interference (SCI), it requires correction for Cross-Channel Interference (XCI) to fully assess NLI. Two correction approaches are compared: a simplified Gaussian Noise (GN)-model-based approximation and the more accurate Polynomial Closed-Form GN/EGN model (PCFM). Experimental validation is conducted over both homogeneous and heterogeneous links, including scenarios with unequal channel power, on two different modulation formats. Results show that while estimation accuracy decreases in complex scenarios, LPM-based methods still provide sufficiently reliable performance for practical optimization tasks, such as determining optimal launch power. These findings support the use of LPM-based NLI estimation as a promising tool for real-time network monitoring and digital twin modeling.**

***Index Terms*—Heterogeneous link, longitudinal power monitoring, optical fiber communications.**

I. Introduction

IN MODERN wideband optical networks, accurate modeling and monitoring are essential for the operation and optimization of the network. In particular, the availability of simple yet effective models of optical network elements, such as optical fibers [1], [2] and Erbium-Doped Fiber Amplifiers (EDFAs) [3], allows building realistic synthetic representations of the network, commonly referred to as digital twins [4]. However, theoretical models rely on several parameters, whose uncertainties can strongly influence their accuracy (and, consequently, the reliability of the digital twin). In the real world, operators rely on multiple sources to obtain these parameters, ranging from the datasheet of the components up to network telemetry data, with different degrees of accuracy.

Among these parameters, a particularly important role is played by those estimated through the receiver's Digital Signal Processing (DSP) [5], using a class of estimation methods broadly known as "Optical Performance Monitoring" (OPM) techniques. Leveraging the receiver's DSP offers clear advantages: the relevant parameters can be estimated by passive monitoring of the signals in the DSP, without requiring any additional hardware. Moreover, these estimations are inherently "end-to-end", as they directly reflect the transmission performance of the Channel of Interest (COI). Current DSP implementations already estimate several parameters, such as Chromatic Dispersion (CD) [6], Polarization-Dependent Loss (PDL) and Polarization Mode Dispersion [7]. Ongoing research indicates that next-generation OPM techniques will further enhance this capability, providing network operators with even richer information [8], such as the power profile [9], I/Q imbalance [10] and fiber length [11].

Other parameters, however, remain significantly more challenging to estimate, such as the separation of noise contributions at the receiver between Amplified Spontaneous Emission (ASE) and Kerr-induced Non-Linear Interference (NLI) [5], [12]. This information is crucial to optimize the optical power of the COI [13], especially in the context of ultra-wideband optical networks [14], [15]. Unfortunately, all of the currently available methods suffer from some serious drawbacks. Time-domain methods [16], [17], [18] suffer from low performance when the NLI power is low. In contrast, frequency-domain [19] or pilot-based [20], [21] approaches are more accurate, but they require modifications in the transmitter. Machine-Learning (ML) methods [22], [23], [24] are robust, but they suffer from generalization problems.

Recently, the use of Linear-Least Squares (LLS) Longitudinal Power Monitoring (LPM) [25] has been proposed [26], [27] to perform this operation. Both theoretical and experimental studies have demonstrated the robustness and accuracy of this approach; however, this method only estimates the NLI power of the *detected channels*. Fortunately, with the ongoing trend towards higher symbol rates [28], [29], the impact of this limitation is expected to decrease in future systems. Nevertheless, this remains a significant limitation (both now and in the near future) that must be addressed to obtain accurate NLI estimates. In [26], all the channels were detected at the receiver, which was feasible because the study was purely numerical and employed

Received 28 October 2025; revised 17 January 2026; accepted 3 February 2026. Date of publication 6 February 2026; date of current version 2 May 2026. This work was supported by CISCO under Sponsored Research Agreement "BOOST 2025". An earlier version of this work was presented in part at the Optical Fiber Communication Conference 2026 Conference [DOI: 10.1364/opticaopen.30394180]. *(Corresponding author: Dario Piloridario.)*

Dario Pilori and Gabriella Bosco are with the Dipartimento di Elettronica e Telecomunicazioni (DET), Politecnico di Torino, 10129 Torino, Italy (e-mail: dario.pilori@polito.it).

Stefano Straullu and Antonino Nespola are with LINKS Foundation, 10138 Torino, Italy.

Stefano Piciaccia is with CISCO Photonics Italy S.r.l., 20871 Vimercate, Italy.

Color versions of one or more figures in this article are available at https://doi.org/10.1109/JLT.2026.3662004.

Digital Object Identifier 10.1109/JLT.2026.3662004

a relatively narrow optical bandwidth. In [27], [30] instead a simplified version of the GN-model [13] was adopted to derive a "correction factor". Although the experimental results were accurate, they were obtained in simple scenarios, in which the rough approximation of the GN-model is known to be accurate.

Therefore, this work extends [31] and aims to provide an extensive and detailed analysis of the accuracy of LPM-based NLI estimation, with a particular focus on heterogeneous links. The technical part of this paper is broadly divided into three Sections. Section II briefly recalls the key principles behind LPM-based NLI estimation and its main limitations. Then, in Section III we present the experimental setup and show results on a short homogeneous link, to demonstrate the capabilities of the setup and the transceiver. The key results are presented in Section IV, where the proposed algorithm is tested on a heterogeneous link composed of mixed G.652 Single-Mode Fiber (SMF) and G.654 Pure-Silica-Core Fiber (PSCF) spans with different length and an unequal transmit power profile. A general discussion on the key results is presented in Section V, and the final conclusions are drawn in Section VI.

II. Principles of the LPM-Based NLI Estimator

This section introduces the principles underlying the LPM-based NLI estimator, describing the extension of LPM to heterogeneous links, the estimation of non-linear SNR from the reconstructed power profile, and the inclusion of correction factors to account for inter-channel non-linear effects.

A. LLS-LPM on a Heterogeneous Link

While the original derivation of the LLS-LPM algorithm [25] assumed a homogeneous link, i.e. a link made of spans of the same fiber type, the algorithm can be easily also applied to heterogeneous links [32], [33]. The LLS-LPM algorithm is based on the following equation [25]

$$\hat{\boldsymbol{\gamma}}' = \left(\mathrm{Re}\left[\boldsymbol{G}^{\dagger}\boldsymbol{G}\right]\right)^{-1}\mathrm{Re}\left[\boldsymbol{G}^{\dagger}\boldsymbol{A}_1\right]\,. \tag{1}$$

This equation depends on two components. The first is the vector $\boldsymbol{A}_1$, which is an estimation of the NLI at the receiver, obtained by subtracting a dispersed version of the transmitted signal from the received signal; this term depends only on the transmitted and received constellations, not on the link itself.

The other is the matrix $\boldsymbol{G}$. According to the first-order regular perturbation (RP1) theory [34], [35], each column represents the effect of chromatic dispersion applied from the input ($z = 0$) to an intermediate distance z_k, followed by a non-linear operator, and then additional dispersion from z_k to the end of the link ($z = L$) [25] [Eq. (8)–(9)]. Consequently, to build this matrix, the link length L must be divided into N steps $[z_0, z_1, \ldots, z_{N-1}]$, and the chromatic dispersion between these steps must be known. In heterogeneous links, this requires full knowledge of the span lengths and the dispersion map, information that may not always be available in practice.

To overcome this limitation, in [36] the authors adopted a different, more practical, approach. Using only the knowledge of the total cumulated dispersion, which is typically estimated by coherent receivers [6], and the total link length L, the link is divided into N uniform steps with spacing $\Delta z = L/N$, determined according to [37]. This results in a power profile that can be "corrected" later, using knowledge of the dispersion parameter and the non-linear coefficient γ of the fiber spans. This applies only if the link is fully uncompensated, i.e. the dispersion map is monotonically increasing. In the presence of fiber spans with a negative dispersion coefficient (e.g., G.655 fiber), the hypotheses of the LLS-LPM are not valid, but – still – a partial power profile may be obtained [32]. However, NLI estimation requires a complete power profile [27]. Therefore, this work focuses only on uncompensated optical links.

B. Non-Linear SNR Estimation

In [27] we proposed to use the byproducts of a LLS-LPM profile to estimate the non-linear SNR, measured at the receiver. In fact, exploiting again the RP1 model, the NLI at the receiver $\hat{\boldsymbol{A}}_1[L, n]$ can be expressed using the estimated power profile $\hat{\boldsymbol{\gamma}}'$ and the $\boldsymbol{G}$ matrix of (1) as:

$$\hat{\boldsymbol{A}}_1[L, n] = \boldsymbol{G}\hat{\boldsymbol{\gamma}}'\,. \tag{2}$$

This equation has the advantage of requiring no prior knowledge of the link or of the non-linear coefficient γ, and it can be directly applied to the uncorrected power profile. Then, from this expression, it is trivial to estimate the non-linear SNR from the Power Spectral Densities (PSDs) of the NLI $\hat{\boldsymbol{A}}_1$ and the reference (i.e., transmitted) signal

$$\mathrm{SNR}_{\mathrm{NL,LPM}} = \frac{G_{A_{\mathrm{ref}}}(0)}{G_{\hat{A}_1}(0)}\,. \tag{3}$$

C. SCI/XCI Correction

The LLS-LPM algorithm inherently estimates only the Self-Channel Interference (SCI) component of the NLI [27], which is the NLI generated by the non-linear beating of the COI with itself [38], [39]. However, there are two other major sources of NLI: Cross-Channel Interference (XCI), which involves the beating between the COI and a single Wavelength Division Multiplexing (WDM) channel, and Multi-Channel Interference (MCI) which represents the beating between more than two WDM channels. Fortunately, MCI is almost negligible for long, uncompensated links with high symbol rate and high dispersion. However, XCI is still a significant NLI source, even if its significance will decrease with the future trend towards higher symbol rates.

Consequently, neglecting MCI, the presence of XCI can be accounted for through a single correction factor, ζ [27]

$$\zeta = \left(1 + \frac{P_{\mathrm{XCI}}}{P_{\mathrm{SCI}}}\right)\,. \tag{4}$$

The advantage of this factor is that it can be directly applied to the non-linear SNR, estimated using (3), obtaining a full estimate of the non-linear SNR

$$\mathrm{SNR}_{\mathrm{NL}} = \mathrm{SNR}_{\mathrm{NL,LPM}}/\zeta\,. \tag{5}$$

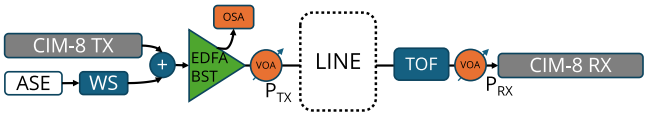

Fig. 1. Schematic of the transmitter and the receiver used in the experimental setup.

The factor ζ can be computed in different ways. In [27], we derived an approximated formula:

$$\log_{10}(\zeta) \approx \frac{1}{4}\log_{10}(N_{\text{ch}}) - 0.0475\left[\log_{10}\left(\frac{B_{\text{L}}}{B_{\text{R}}}\right)\right]^2. \quad (6)$$

In this equation, N_{ch} is the total number of WDM channels, B_{L} and B_{R} are, respectively, the optical bandwidth at the left and at the right of the COI.

This approximation yielded surprisingly good results in the scenarios considered in that work. However, it relies on a coarse GN-model approximation [13], [40], which assumes a perfectly homogeneous link, and a uniform WDM comb, in which all channels are identical and with the same optical power. Therefore, in realistic scenarios, this approximation might not give accurate results. Instead, when all link parameters are known, an exact value of ζ can be obtained using a full NLI model, such as the Polynomial Closed-Form GN-EGN Model (PCFM) [1]. Since it explicitly separates SCI and XCI components [1] [Eq. (1)], ζ can be directly computed from P_{XCI} and P_{SCI} using (6). For instance, a publicly-available software implementation of the PCFM [41] is able to compute separately the power of SCI and XCI.

In this work, we compare the NLI estimation accuracy obtained using these two different techniques for computing ζ: the rough approximation of (4), and the value derived from the PCFM, which is considered as the ground truth. This comparison is key to measure the real accuracy of the LPM-based NLI estimation.

III. Homogeneous Link

This section presents the experimental validation of the algorithm over a simple and short homogeneous link composed solely of SMF. Compared to the results reported in [27], the new experiments were performed at a higher symbol rate, using hard-decision to generate the reference signal. While the main focus of this paper is on heterogeneous links, the purpose of this section is to provide a benchmark for the algorithm, as the same transceiver was used in the heterogeneous-link experiments reported in Section IV.

A. Experimental Setup

A schematic of the experimental transmitter and receiver setup is shown in Fig. 1. At the transmitter, the COI was generated using a commercial transceiver (CISCO CIM-8 equipped with Acacia's JANNU DSP) operating at ~ 118 GBaud. The modulation format was Polarization-Multiplexed (PM) 16- Quadrature-Amplitude Modulation (QAM). The other WDM channels,

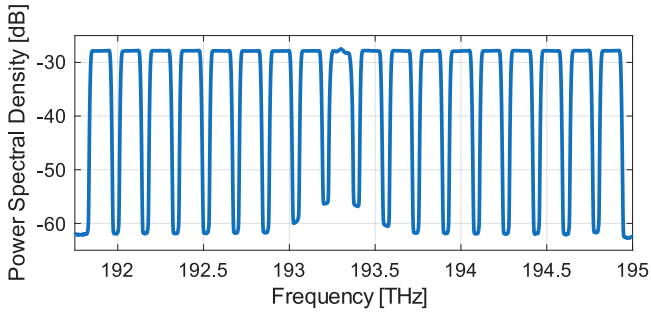

Fig. 2. Transmit optical spectrum, where the central channel (193.3 THz) was modulated with a commercial transceiver, and the other channels were emulated by shaped ASE noise.

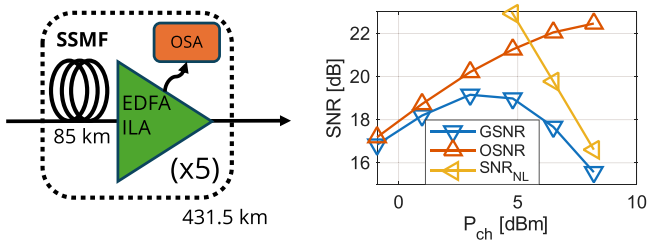

(a) (b)

Fig. 3. (a) Schematic of the link, with the same transmitter and receiver of Fig. 1. (b) GSNR (extracted from the card's BER) and OSNR (measured with an OSA over the signal's bandwidth) of the central WDM channel (193.3 THz), as function of the per-channel transmit power P_{ch}. The non-linear SNR is computed from those two values.

spaced by 175 GHz, were emulated using Amplified Spontaneous Emission (ASE) noise, spectrally shaped by a WaveShaper (WS) [42], [43]. The transmitted optical spectrum, measured by an Optical Spectrum Analyzer (OSA), is shown in Fig. 2. A booster (BST) EDFA amplifier, followed by a Variable Optical Attenuator (VOA) was used to set a per-channel transmit power into the line. After transmission, the COI was selected using a tunable optical filter (TOF) and detected by the real-time DSP of the CIM-8 transceiver. From the transceiver telemetry data, we captured the average Bit Error Ratio (BER) and the cumulated chromatic dispersion (CD), as estimated by the card, as well as 100 constellation blocks, each 12 288 symbols long. Each block was then used as input to the LLS-LPM algorithm, followed by NLI estimation. The estimated non-linear SNR values for each block were averaged to obtain the final result. The reference signal was generated by taking hard decisions on the received constellation, after applying a correction factor based on the BER [44].

First, we tested the transceiver performance over a short, homogeneous, link, made of 5×85-km spans of SMF, with EDFA amplification. A schematic of the link setup is shown in Fig. 3(a), and the results for the central WDM channel are shown in Fig. 3(b). The figure reports the Generalized SNR (GSNR) [45] (i.e., the card's SNR after removing the back-to-back penalty) and the OSNR at the receiver, computed over the signal's bandwidth. The measured non-linear SNR, used as benchmark for the LPM-based estimation method, was

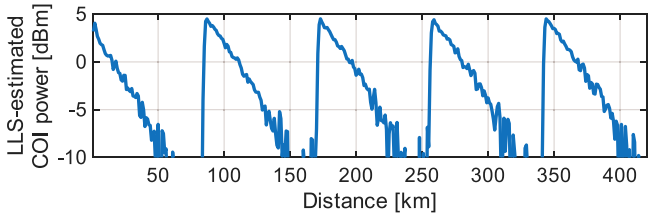

Fig. 4. Estimated power profile of the 5×85-km SMF link, computed at a transmit power close to the optimal one, for the central WDM channel (193.3 THz).

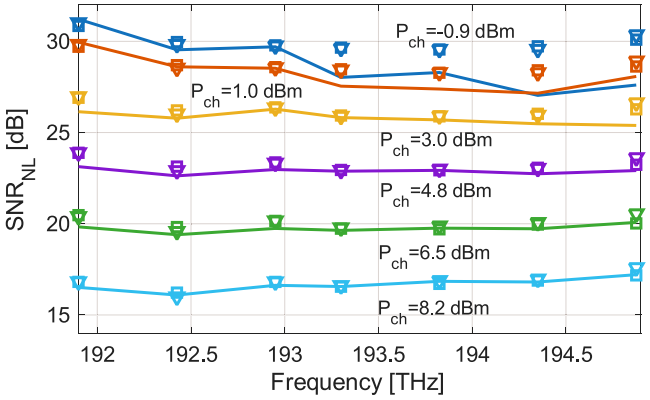

Fig. 5. Validation of the non-linear SNR estimation over the 431-km SMF link. Solid line: Measured value with (7). Markers: LPM estimation using either the approximated XCI correction formula of (6) (squares), or the PCFM (triangles). Different colors correspond to different per-channel transmit power values P_{ch}.

computed (in linear units) as

$$\frac{1}{\text{SNR}_{\text{NL}}} = \frac{1}{\text{GSNR}} - \frac{1}{\text{OSNR}}. \tag{7}$$

This expression assumes that the NLI affecting the final constellation behaves as Gaussian-distributed noise [39], which means that the Kerr-induced Phase and Polarization Rotation Noise (PPRN) [38] is effectively compensated by the receiver's DSP. The optimal per-channel transmit power is approximately $+4.5$ dBm. It is worth noting that, due to the short link length, the OSNR saturates at high transmit powers, due to the ASE noise added by the transmitter (mainly the booster amplifier).

B. NLI Estimation Results and Discussion

The LLS-LPM algorithm was applied to the blocks of received signal samples recorded by the CIM-8 transceiver with a 1-km spatial resolution to generate the power profile of the link. The result, for a transmitted power of approximately 4.8 dBm, is shown in Fig. 4. As expected, the profile clearly shows the power evolution of the channel, with a lower accuracy in the first span, due to the non-Gaussian shape of the transmitted constellation [37].

The estimated power profile and the $\boldsymbol{G}$ matrix of the algorithm were then used to compute the non-linear SNR. The results are shown as markers in Fig. 5, where each color corresponds to a different transmit optical power, and the purple line (fourth from the top) is close to the optimal transmit power. The COI's

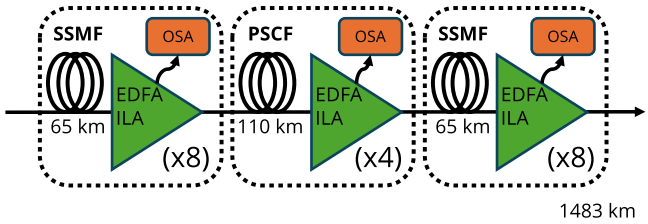

Fig. 6. Schematic of the link, made of 8×65-km spans of SMF, followed by 4×110-km spans of PSCF, and then another 8×65 -km spans of SMF, for a total length of approximately 1483 km.

frequency was changed to measure the NLI for 7 WDM channels, distributed along the WDM comb, while the other channels were generated with shaped ASE noise. Squares indicate values obtained using ζ computed with the approximated formula in (6), while triangles represent values obtained using ζ computed with the PCFM [1] NLI model. As benchmark, the solid lines show the non-linear SNR computed using (7). It should be noted that for the lowest power levels (blue and red curves and markers), the benchmark results are less reliable due to the very low (absolute) NLI power. Nevertheless, the results around the optimal transmit power are accurate, and the difference between the XCI approximation and the PCFM is very small. As expected, these results are consistent with those reported in [27], which were obtained on a similar link but using a different transmitter.

IV. Heterogeneous Link

After validating the proposed algorithm on a simple homogeneous setup, we further evaluated its performance in a more challenging heterogeneous scenario. The tested link consisted of a mix of different fiber types and included cases with non-uniform transmit power distribution. The experimental setup and corresponding results are described in the following.

A. Experimental Setup

The schematic of the heterogeneous transmission scenario is shown in Fig. 6. The link mixes G.652 SMF fibers with G.654 PSCF fibers, characterized by different values of γ and β_2. Due to the lower GSNR of this link configuration compared to the homogeneous link in Section III, the PM-QPSK format was used for the COI in this experiment. After propagation and detection, we applied the LLS-LPM algorithm to the received signal samples, yielding the power profiles shown in Fig. 7. In the figure, the yellow dashed line corresponds to the power profile obtained under the assumption of a homogeneous link. It can be observed that both the span length and the power are not correct because of the differences in dispersion and effective area between SMF and PSCF. If the parameters of the fiber spans are known, the profile can be corrected, by applying a different span-per-span scaling factor on the distance and power axes, [33] to obtain the blue solid curve. The span parameters, which were obtained either from direct measurements (attenuation and dispersion) or from datasheets (effective area), are summarized in Table I. It is important to note that the correction is needed only for the evaluation of the power profile and not for the

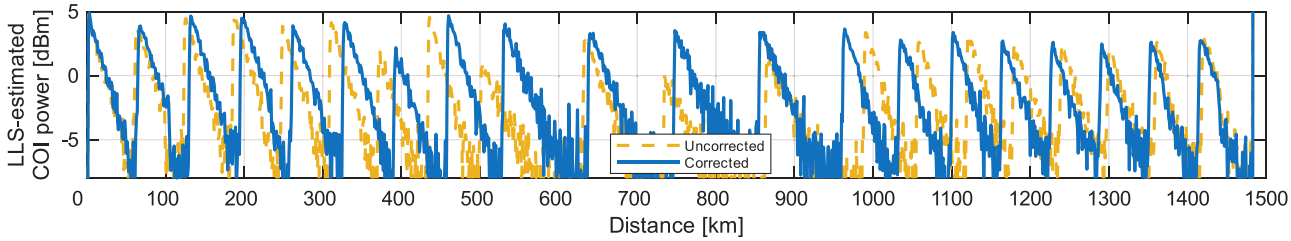

Fig. 7. Estimated power profile of the 1483-km heterogeneous link. The yellow dashed line corresponds to the uncorrected power profile, i.e. obtained without knowledge of the link. The blue solid line represents the same profile, after correction using the dispersion map.

TABLE I
LINK FIBER PARAMETERS AT 193.3 THZ

Span	Type	L [km]	D_λ [ps/(nm · km)]	A_{eff} [μm^2]
1	SMF	65.36	16.40	80
2	SMF	65.22	16.60	80
3	SMF	65.02	16.58	80
4	SMF	65.30	16.47	80
5	SMF	65.10	16.44	80
6	SMF	65.61	16.40	80
7	SMF	67.22	16.44	80
8	SMF	70.97	16.37	80
9	PSCF	108.83	20.92	130
10	PSCF	108.94	16.40	86
11	PSCF	108.88	20.70	150
12	PSCF	106.36	20.50	110
13	SMF	70.86	16.44	80
14	SMF	67.38	16.47	80
15	SMF	62.89	16.25	80
16	SMF	62.89	16.60	80
17	SMF	62.85	16.60	80
18	SMF	62.84	16.80	80
19	SMF	62.88	16.50	80
20	SMF	67.80	16.18	80

NLI estimation. Indeed, NLI estimation was performed on both corrected and uncorrected profiles, obtaining identical results. Therefore, all power profiles used in the following analysis correspond to the uncorrected case.

Similarly to the previous setup, we also measured the GSNR and the OSNR (measured over the signal's bandwidth), and we computed the non-linear SNR using (7). The results are shown in Fig. 8. Because of the limited output power of the EDFAs, it was not possible to reach very high values of transmit optical power. Nevertheless, we were able to fully capture the optimal transmit power, which was around $+5.5$ dBm. Note that, due to the longer distance, in this experiment the OSNR did not saturate at high values of optical power.

B. Non-Linear SNR Estimation

The estimated non-linear SNR for this link is shown in Fig. 9, where different colors correspond to different transmit power values, and the purple line (third from top) is close to the optimal power. Compared to the previous results (see Fig. 5), the accuracy is lower. This is expected, since the scenario is more challenging: there is a significant power difference between the channels at the end of the link (the link does not contain any WSS), and the power profile of Fig. 7 is noisier. Nevertheless, the performance is still good, with a negligible difference between the two XCI estimation algorithms.

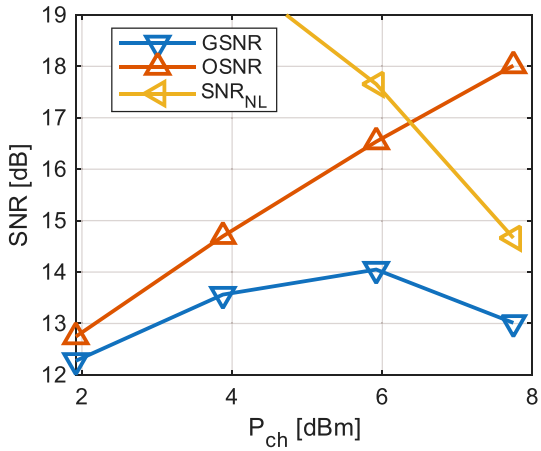

Fig. 8. Measured values of GSNR and OSNR (measured over the signal's bandwidth), and computed non-linear SNR for the heterogeneous-link experiment.

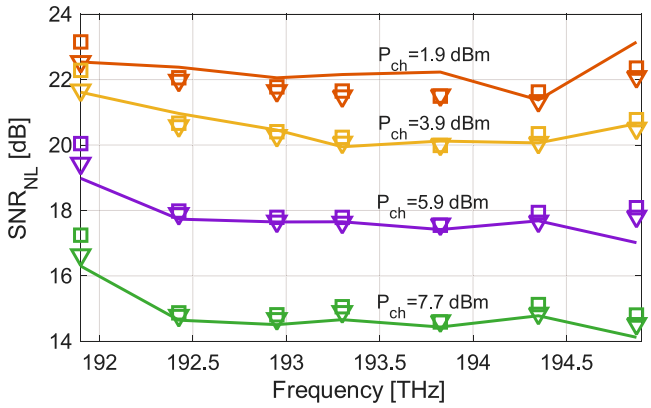

Fig. 9. Validation of the non-linear SNR estimation over the 1483-km heterogeneous link. Solid line: Measured value with (7). Markers: LPM estimation using either the approximated XCI correction formula of (6) (squares), or the PCFM (triangles). Different colors correspond to different per-channel transmit power values P_{ch}.

C. Unequal Channel Power

For the derivation of the approximated expression of ζ in (6), two key assumptions were made: both the link and the WDM

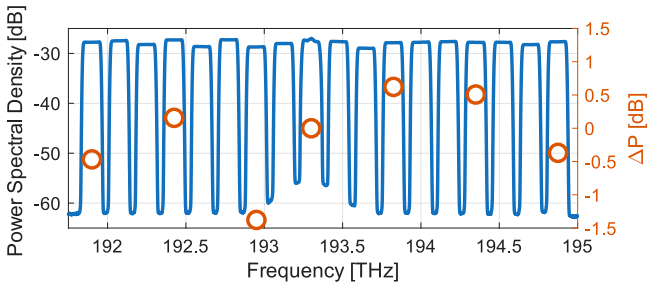

Fig. 10. Transmit optical spectrum with unequal power among the WDM channels (blue line, left axis). The power difference with respect to the central WDM channel is highlighted by the red circles (right axis).

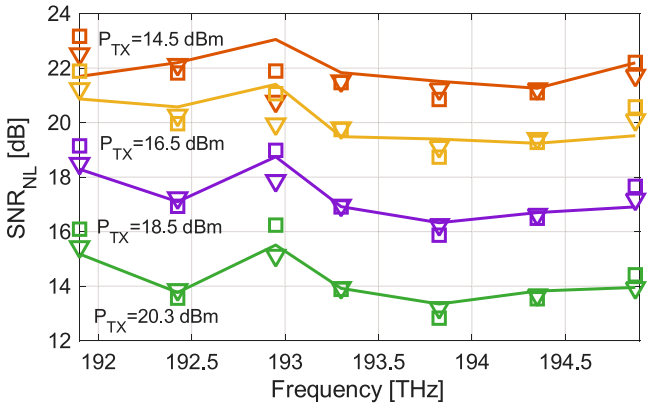

Fig. 11. Validation of the non-linear SNR estimation over the 1483-km heterogeneous link with an unequal launch power profile. Solid line: Measured value with (7). Markers: LPM estimation using either the approximated XCI correction formula of (6) (squares), or the PCFM (triangles). Different colors correspond to different total transmit power P_{TX} values.

comb must be homogeneous. As shown in the previous subsection, that approximation works also in a heterogeneous link composed of different fiber types and span lengths. However, in that case the WDM channels had equal launch power. To evaluate the impact of power imbalance, we introduced random per-channel variations uniformly distributed in the range $[-1.5, +1.5]$ dB, resulting in the transmit optical spectrum shown in Fig. 10 (left axis). The right axis (red circles) highlights, on a smaller scale, the power difference between channels, using – as a reference – the central WDM channel. The chosen imbalance was large enough to have an impact on XCI, while remaining within realistic operational limits. The transmission was tested over the same 1483-km heterogeneous link described in the previous section.

The estimated non-linear SNR values (markers), compared with the measurements (solid lines), are shown in Fig. 11. In contrast to previous Figures, the legend shows the total (and not the per-channel) power, since it is different for each WDM channel.

In this case, the difference between the results obtained using (6) (squares) and those computed with the PCFM model (triangles) is greater, especially for the channel with the largest power deviation (192.95 THz). Despite this, the proposed estimation method maintains good accuracy, with errors typically below 1 dB across the tested frequency range and launch powers. These results confirm its suitability for practical deployment in realistic optical systems.

V. Discussion

Based on the results described in this paper, together with those in [27], it can be concluded that the LLS-LPM algorithm provides reliable SCI estimation under typical conditions where NLI behaves as an AWGN source (i.e., when (7) is valid). A noisier reconstructed power profile is expected to reduce SCI estimation accuracy, as discussed in [37], and this aspect deserves further investigation. Even so, since (almost) all optical networks use WDM, a detailed study on SCI estimation alone would have limited real-world impact.

Regarding the XCI estimation, this work demonstrates that in "normal" conditions, the simple approximation of (6) holds. By "normal", we refer to systems with approximately uniform WDM combs (equal symbol rate and spacing, and mild power differences among channels). However, when the power difference is larger, for instance for the channel at 192.95 THz in Fig. 11, the performance of the NLI estimation algorithm slightly decreases. This is expected, since (6) was derived (following [40]) assuming a perfectly homogeneous link and WDM comb. In this case, a full NLI model can provide more accurate results, at the expense of requiring knowledge of all system parameters. However, as shown in Fig. 11, even PCFM predictions exhibit some deviations. These are likely due to parameter uncertainties and the limited precision of reference measurements. Mainly, they originate from the GSNR and OSNR values used in (7), whose combined measurement errors distort the reference curves at low power, as seen in Fig. 9. However, the main purpose of non-linear SNR estimation is usually to determine the optimal transmit power [13], which depends (in dB scale) on the non-linear SNR scaled by a factor of $1/3$. Consequently, this scaling strongly mitigates the impact of these inaccuracies on the estimated optimal power.

Three main experimental constraints should also be noted. First, the channel spacing was relatively large. This was necessary to accurately measure the OSNR, which is needed to obtain the reference curves (solid lines in Figs. 5, 9, and 11). However, this reduces the amount of XCI affecting the channels; consequently, the measured XCI contribution was slightly smaller than in typical dense-WDM scenarios.

The second limitation concerns the modulation format. In this work, we transmitted QPSK and 16-QAM. On one hand, these modulation formats produce noisier power profiles [37]; on the other, they induce less PPRN, which facilitates the estimation of non-linear noise. However, all interfering channels were generated by shaped ASE noise [42], [43], corresponding to a Gaussian constellation [38], [46] which induces stronger PPRN and XCI. Hence, we believe that, using a Gaussian-like constellation (e.g., QAM with probabilistic constellation shaping) on all WDM channels, would yield similar results. Future studies should also investigate denser channel grids, higher-order modulation formats, and dynamic network scenarios to further assess the applicability of LPM-based NLI estimation.

Finally, the third limitation is the overall optical bandwidth. This experiment was carried out using only (part of) the C-band. Future multi-band systems, using also the L- (and possibly other) bands [47], exhibit strong Inter-channel Stimulated Raman Scattering (ISRS), which adds a power transfer between the channels. While the LPM algorithm was extensively tested on those scenarios [48], [49], NLI estimation was never attempted. In general, given the accuracy of LPM in the presence of ISRS, we can assume that SCI estimation would be still accurate. However, the computation of the correction coefficient ζ might be different, especially when using models – such as (6) – that do not consider ISRS. Consequently, the overall estimation of NLI might require different – and more complex – expressions of ζ, and this is also left for future investigations.

VI. Conclusion

NLI estimation based on LPM is a powerful and robust technique, which does not require any prior knowledge of the link configuration. However, it has a significant limitation: it estimates only a portion of the total NLI, namely the Self-Channel Interference. In this work, we investigated the performance of LPM-based NLI estimation in three different experimental scenarios, focusing on the accuracy of the SCI/XCI ratio, which is needed to estimate the full NLI power at the receiver. We adopted a simple approximation based on the GN-model, and, as benchmark, we used a recently-published full NLI model: the PCFM. The approximation assumes a homogeneous link and a uniform WDM transmission. Therefore, we accurately tested its behavior on two cases: a heterogeneous link, mixing SMF and PSCF fiber of different lengths, and a non-uniform WDM comb, with a power imbalance among channels. As expected, the accuracy of NLI estimation in a heterogeneous link is lower, especially in the presence of a power imbalance between the channels. Nevertheless, the method still achieved satisfactory performance. Consequently, we believe that these results show that this method is a promising technique for monitoring and optimization of optical networks, which can be applied in conjunction with power profile estimation.

Acknowledgment

The authors would like to thank Yanchao Jiang and Pierluigi Poggiolini for their help on using the PCFM model, Lorenzo Andrenacci and Fabrizio Forghieri for useful discussions.

References

[1] P. Poggiolini and Y. Jiang, "Recent advances in real-time models for multiband transmission systems," in *Proc. Opt. Fiber Commun. Conf. 2025*, 2025, pp. 1–3.

[2] H. Buglia, R. I. Killey, and P. Bayvel, "Ultra-wideband modeling of optical fibre nonlinearity in hybrid-amplified links," *J. Lightw. Technol.*, vol. 42, no. 24, pp. 8664–8677, Dec. 2024.

[3] Y. Liu et al., "Building a digital twin of an EDFA for optical networks: A gray-box modeling approach," *J. Opt. Commun. Netw.*, vol. 15, no. 11, pp. 830–838, Nov. 2023.

[4] D. Wang et al., "Digital twin of optical networks: A review of recent advances and future trends," *J. Lightw. Technol.*, vol. 42, no. 12, pp. 4233–4259, Jun. 2024.

[5] M. S. Faruk and S. J. Savory, "Measurement informed models and digital twins for optical fiber communication systems," *J. Lightw. Technol.*, vol. 42, no. 3, pp. 1016–1030, Feb. 2024.

[6] C. Malouin, P. Thomas, B. Zhang, J. O'Neil, and T. Schmidt, "Natural expression of the best-match search godard clock-tone algorithm for blind chromatic dispersion estimation in digital coherent receivers," presented at the *Adv. Photon. Congr.*, Colorado Springs. CO, USA, Jun. 9–21, 2012, Paper SpTh2B.4.

[7] M. S. Faruk, Y. Mori, C. Zhang, K. Igarashi, and K. Kikuchi, "Multi-impairment monitoring from adaptive finite-impulse-response filters in a digital coherent receiver," *Opt. Exp.*, vol. 18, no. 26, pp. 26929–26936, Dec. 2010.

[8] P. Layec, C. Delezoide, K. Abdelli, and F. Boitier, "Sensing, learning, and protecting optical networks," in *Proc. Opt. Fiber Commun. Conf. 2025*, 2025, pp. 1–3.

[9] M. R. Sena et al., "Link tomography: A tool for monitoring optical network and designing digital twins," in *Proc. 50th Eur. Conf. Opt. Commun.*, 2024, pp. 176–179.

[10] K. Zhang, J. Li, T. Ye, H. Nakashima, T. Hoshida, and Z. Tao, "In-service monitor and pre-compensation of 100 Gbaud-class coherent transmitter by a 5 GHz photodetector," in *Proc. Opt. Fiber Commun. Conf. 2025*, 2025, pp. 1–3.

[11] N. Campos, M. Olmos, A. M. Balsa, and D. Morero, "A modulation-agnostic pilot-aided fiber length estimator for high-speed coherent links," in *Proc. Opt. Fiber Commun. Conf. 2025*, 2025, pp. 1–3.

[12] D. Pilori, L. Andrenacci, and G. Bosco, "Estimating the nonlinear interference at the receiver: Methods and pitfalls," presented at the *Adv. Photon. Congr.*, Marseille, France, Jul. 13–17, 2025, Paper SpTh2F.3.

[13] P. Poggiolini, G. Bosco, A. Carena, V. Curri, Y. Jiang, and F. Forghieri, "The GN-model of fiber non-linear propagation and its applications," *J. Lightw. Technol.*, vol. 32, no. 4, pp. 694–721, Feb. 2014.

[14] H. Buglia, E. Sillekens, A. Vasylchenkova, P. Bayvel, and L. Galdino, "On the impact of launch power optimization and transceiver noise on the performance of ultra-wideband transmission systems [invited]," *J. Opt. Commun. Netw.*, vol. 14, no. 5, pp. B11–B21, May 2022.

[15] Y. Jiang, F. Forghieri, S. Piciaccia, G. Bosco, and P. Poggiolini, "Optimum launch power in multiband systems," in *Proc. 50th Eur. Conf. Opt. Commun.*, 2024, pp. 930–933.

[16] F. J. Caballero et al., "Machine learning based linear and nonlinear noise estimation," *J. Opt. Commun. Netw.*, vol. 10, no. 10, pp. D42–D51, Oct. 2018.

[17] D. Lippiatt, S. Varughese, T. Richter, S. Tibuleac, and S. E. Ralph, "Joint linear and nonlinear noise estimation of optical links by exploiting carrier phase recovery," in *Proc. Opt. Fiber Commun. Conf. Exhib.*, 2020, pp. 1–3.

[18] G. D. Rosa, S. Dris, and A. Richter, "Statistical quantification of nonlinear interference noise components in coherent systems," *Opt. Exp.*, vol. 28, no. 4, pp. 5436–5447, Feb. 2020.

[19] F. J. Vaquero-Caballero, D. J. Ives, and S. J. Savory, "Perturbation-based frequency domain linear and nonlinear noise estimation," *J. Lightw. Technol.*, vol. 40, no. 18, pp. 6055–6063, Sep. 2022.

[20] C. Rasmussen and M. Aydinlik, "Optical signal-to-noise ratio (OSNR) monitoring and measurement in optical communications sytems," U.S. Patent 9,847,833, Dec. 19, 2017.

[21] S. Searcy, G. He, and S. Tibuleac, "Experimental validation of GOSNR estimation using polarization-resolved optical spectrum analysis on metro and long-haul WDM links," in *Proc. Opt. Fiber Commun. Conf. 2025*, 2025, pp. 1–3.

[22] H. J. Cho et al., "Constellation-based identification of linear and nonlinear OSNR using machine learning: A study of link-agnostic performance," *Opt. Exp.*, vol. 30, no. 2, pp. 2693–2710, 2022.

[23] M. Al-Nahhal, I. Al-Nahhal, O. A. Dobre, and S. K. O. Soman, "Parallel neural network structures for signal-to-noise ratio estimation in optical fiber communication systems," *J. Lightw. Technol.*, vol. 42, no. 6, pp. 1941–1954, Mar. 2024.

[24] M. Boertjes, A. S. Kashi, J. C. Cartledge, and W.-Y. Chan, "Machine learning model training framework for nonlinear signal-to-noise ratio estimation in heterogeneous optical networks," *J. Lightw. Technol.*, vol. 42, no. 14, pp. 4789–4799, Jul. 2024.

[25] T. Sasai, M. Takahashi, M. Nakamura, E. Yamazaki, and Y. Kisaka, "Linear least squares estimation of fiber-longitudinal optical power profile," *J. Lightw. Technol.*, vol. 42, no. 6, pp. 1955–1965, Mar. 2024.

[26] I. Kim, K. Sone, O. Vassilieva, S. Oda, P. Palacharla, and T. Hoshida, "Nonlinear SNR estimation based on power profile estimation in hybrid Raman-EDFA link," in *Proc. Opt. Fiber Commun. Conf. 2024*, 2024, pp. 1–3.

[27] L. Andrenacci, G. Bosco, Y. Jiang, A. Nespola, S. Piciaccia, and D. Pilori, "DSP-based nonlinear interference estimation using linear least squares longitudinal power monitoring," *J. Lightw. Technol.*, vol. 43, no. 8, pp. 3536–3546, Apr. 2025.

[28] C. Deakin, X. Chen, G. Raybon, and D. Che, "440-GBaud all-electronic signaling enabling single-wavelength net rate over 1 Tb/s per modulation dimension," presented at the *Opt. Fiber Commun. Conf.* San Francisco, CA, USA, Mar. 30–Apr. 3, 2025, Paper Th4B.7.

[29] D. Drayß et al., "Optical arbitrary waveform generation (OAWG) using actively phase-stabilized spectral stitching," *Light, Sci. Appl.*, vol. 14, no. 1, 2025, Art. no. 353.

[30] L. Andrenacci et al., "Nonlinear noise estimation using linear least squares-based longitudinal power monitoring," in *Proc. 50th Eur. Conf. Opt. Commun.*, 2024, pp. 172–175.

[31] D. Pilori, S. Straullu, A. Nespola, L. Andrenacci, S. Piciaccia, and G. Bosco, "Accuracy of LPM-based NLI estimation over a heterogeneous link," in *Proc. Opt. Fiber Commun. Conf.*, Los Angeles Mar. 2026, Paper W2A.49.

[32] D. Pilori, S. Straullu, A. Nespola, L. Andrenacci, S. Piciaccia, and G. Bosco, "Experimental demonstration of longitudinal power monitoring over a mixed fiber link," *IEEE Photon. Technol. Lett.*, vol. 37, no. 20, pp. 1181–1184, Oct. 2025.

[33] M. Takahashi, T. Sasai, and E. Yamazaki, "Fiber characterization and longitudinal power monitoring in heterogeneous fiber link," in *Proc. 30th OptoElectronics Commun. Conf. 2025 Int. Conf. Photon. Switching Comput.*, 2025, pp. 1–4.

[34] A. Vannucci, P. Serena, and A. Bononi, "The RP method: A new tool for the iterative solution of the nonlinear schrodinger equation," *J. Lightw. Technol.*, vol. 20, no. 7, pp. 1102–1112, Jul. 2002.

[35] P. Serena and A. Bononi, "An alternative approach to the Gaussian noise model and its system implications," *J. Lightw. Technol.*, vol. 31, no. 22, pp. 3489–3499, Nov. 2013.

[36] M. Takahashi, T. Sasai, M. Nakamura, and E. Yamazaki, "Experimental investigation of longitudinal power profile estimation accuracy in fibre links with large effective core area," in *Proc. 50th Eur. Conf. Opt. Commun.*, 2024, pp. 990–993.

[37] T. Sasai, S. Y. Set, and S. Yamashita, "Design of fiber-longitudinal optical power monitor," *J. Lightw. Technol.*, vol. 43, no. 5, pp. 2192–2202, Mar. 2025.

[38] R. Dar, M. Feder, A. Mecozzi, and M. Shtaif, "Properties of nonlinear noise in long, dispersion-uncompensated fiber links," *Opt. Exp.*, vol. 21, no. 22, pp. 25685–25699, Nov. 2013.

[39] P. Poggiolini, "The GN model of non-linear propagation in uncompensated coherent optical systems," *J. Lightw. Technol.*, vol. 30, no. 24, pp. 3857–3879, Dec. 2012.

[40] V. Curri et al., "Design strategies and merit of system parameters for uniform uncompensated links supporting Nyquist-WDM transmission," *J. Lightw. Technol.*, vol. 33, no. 18, pp. 3921–3932, Sep. 2015.

[41] Y. Jiang and P. Poggiolini, "Optical link performance calculator based on the polynomial closed-form GN/EGN model (PCFM)," 2025, doi: 10.5281/zenodo.16412649.

[42] D. J. Elson et al., "Investigation of bandwidth loading in optical fibre transmission using amplified spontaneous emission noise," *Opt. Exp.*, vol. 25, no. 16, pp. 19529–19537, Aug. 2017.

[43] T. Richter, J. Pan, and S. Tibuleac, "Comparison of WDM bandwidth loading using individual transponders, shaped, and flat ASE noise," in *Proc. Opt. Fiber Commun. Conf.*, 2018, pp. 1–3.

[44] L. Andrenacci et al., "Implementation penalties for nonlinear interference estimation with linear least squares longitudinal power monitoring," in *Proc. Opt. Fiber Commun. Conf. 2025*, 2025, pp. 1–3.

[45] E. R. Hartling, "From the acceptance of turnkey systems to open networks with G-SNR," in *Proc. Opt. Fiber Commun. Conf. 2020*, 2020, pp. 1–28.

[46] A. Carena, G. Bosco, V. Curri, Y. Jiang, P. Poggiolini, and F. Forghieri, "EGN model of non-linear fiber propagation," *Opt. Exp.*, vol. 22, no. 13, pp. 16335–16362, Jun. 2014.

[47] S. Shimizu et al., "27-THz ISRS-supported transmission over 1040 km in S+C+L+U and extreme longer-wavelength band," in *Proc. Opt. Fiber Commun. Conf. Postdeadline Papers 2025*, 2025, pp. 1–3.

[48] L. Andrenacci et al., "Experimental demonstration of linear least squares-based longitudinal power monitoring over a raman-amplified C+L link," in *Proc. 50th Eur. Conf. Opt. Commun.*, 2024, pp. 503–506.

[49] R. Kaneko, T. Sasai, M. Nakamura, F. Hamaoka, and E. Yamazaki, "Visualizing longitudinal evolution of forward- and backward-Raman-amplified power and gain," in *Proc. Opt. Fiber Commun. Conf. Exhib.*, 2025, pp. 1–3.